

Interaction of water with clean and oxygen precovered nickel surfaces

M. Schulze¹, R. Reißner¹, K. Bolwin¹, W. Kuch²

¹Deutsche Forschungsanstalt für Luft- und Raumfahrt (DLR), Institut für Technische Thermodynamik, Pfaffenwaldring 38-40, D-70679 Stuttgart, Germany

²MPI für Mikrostrukturphysik, Labor für Synchrotron strahlung, Takustrasse 11 D-14135 Berlin, Germany

Received: 3 April 1995/Accepted: 2 May 1995

Abstract. The adsorption of water on a Ni(111) single crystal surface, clean as well as precovered with oxygen, has been investigated with thermal desorption spectroscopy (TDS) and measurements of the adsorption-desorption equilibrium combined with XPS (X-ray photoelectron spectroscopy). The measurements have been carried out with water pressures up to 10^{-5} mbar on surfaces, which have been either clean or precovered with oxygen. On the clean Ni(111) surface the first adsorbate layer with a maximum coverage of 0.42 ML (monolayers) has a desorption energy of 52 kJ/mol and a preexponential factor of desorption of 10^{16} s⁻¹. A second water layer adsorbs with the desorption energy of the ice multilayer but with first order kinetics. On Ni(111) precovered with chemisorbed oxygen an additional state of molecular, more strongly bound water is found, but no dissociation. For higher oxygen precoverages where NiO islands are formed on the surface, also the water dissociation product OH is found adsorbed. On a sample covered with a closed NiO layer, adsorbed OH and molecular water in an energetically not well-defined state are found. High doses of water on oxygen-precovered Ni(111) induce a slow surface modification leading to water dissociation.

Introduction

The important reaction steps of electrocatalytic processes take place at the solid-liquid interface between a metal electrode and an electrolytic solution. Nickel is commonly used as catalyst in aqueous electrolytes in water electrolysis and fuel cells. In recent years simulation experiments in ultrahigh vacuum (UHV) have been performed in order to obtain reliable information about the binding properties at these interfaces.

Here the adsorption and desorption of H₂O is investigated on clean and with oxygen precovered as well as on the oxidized Ni(111) surface: For adsorption of H₂O on

hexagonal surfaces a so-called bilayer structure is a frequently used model: one half of the first adsorbate layer is bonded directly to the metal surface by the oxygen atoms; the other half of the adsorbate layer is bonded to the first half of the layer by means of hydrogen bonds. This structure is based on the bulk structure of ice. Up to now a long range order in the submonolayer regime could only be proved for ruthenium [1]. For Ni(111) the misfit of the lattice of the ice structure amounts to -0.02 nm.

With the coadsorption of H₂O and O, some metals cause a dissociation of the water [1–3]. On the pure Ni(111) surface as well as in the presence of chemisorbed oxygen, only molecular water was found [4–7]. Steps or defects on the Ni(111) surface on the other hand result in a dissociation of water, due to a charge transfer occurring on the steps [8]. Thus the surface behaves similarly to a surface that is precovered with alkali atoms [5–9]. The defect density of a NiO layer also seems to have a strong influence on the dissociation of H₂O [1, 10].

The desorption energy data reported for H₂O on the clean Ni(111) surface, obtained by TDS-measurements, vary between $E = 41$ kJ/mol [11] and $E = 57$ kJ/mol [4]. Theoretical cluster calculations show activation energies between $E = 51.4$ kJ/mol and $E = 67.1$ kJ/mol [12]. An attractive lateral interaction between water molecules ranges at the most from 1 to 2 kJ/mol [1, 5, 11, 13]. Accordingly, for the ice multilayer, a value of $E = 48$ kJ/mol [11] for the desorption energy results from TDS measurements and a value of 38 kJ/mol [14] from measurements of the isothermal desorption.

Experimental

Experiments were carried out in a standard UHV chamber equipped with a spherical electron analyzer ($R = 127$ mm), an X-ray source with Mg- and Al-anodes, a LEED system, a mass spectrometer, an H₂O molecular beam and devices for standard sample preparation. The latter are described in reference [7]. Ultrapure water was used, which was further purified by cycles of freezing, pumping and thawing. A nickel single crystal was used as sample, the surface of which was checked routinely by XPS and LEED after preparation.

The desorption of H₂O was investigated using X-ray photoelectron spectroscopy (XPS) in dynamic adsorption-desorption equilibrium. The adsorption flux onto the surface was set up with a H₂O molecular beam, resulting in an H₂O-partial pressure of 10^{-7} to 2×10^{-5} mbar at the

surface, i. e., the H_2O flux onto the surface is equal to the particle flux at a pressure of 10^{-7} to 10^{-5} . The flux in the H_2O beam was determined using a Pitot-tube and by comparison of adsorption measurements at 100 K with water exposure by the H_2O molecular beam and diffuse water exposure. The overall pressure in the analysis chamber did not exceed 10^{-9} mbar. The adsorption flux is defined through the particle flux onto the surface and the sticking coefficient S . Equilibrium curves of water coverage versus the incident water beam intensity were taken at various temperatures in the range of 155–175 K, stopping the water beam flux after acquisition of each single data point and allowing the adsorbed water to desorb. For a given H_2O flux onto the sample a certain equilibrium coverage $\Theta_{\text{H}_2\text{O}}$ adjusts itself, provided that the desorption rate depends upon coverage. The adsorption flux is the product of sticking probability S and the particle flux j that hits the surface. The sticking coefficient was derived by adsorption measurements at 100 K. The water coverage on the surface was increased linearly in time and no saturation was observed. The water was dosed by a leak valve and alternatively by using the H_2O molecular beam; both gives a constant sticking coefficient $S = 1$. Thus the water adsorption on Nickel is not activated or the activation energy is so low, that we could not find any evidence for an activation in the considered temperature range and we found no evidence that the sticking coefficient depends on temperature. The desorption flux is determined by the coverage Θ and the desorption coefficient D . From the measured coverages Θ and the experimentally adjusted desorption flux the temperature- and coverage-dependent desorption coefficient D is determined by the equation $jS = j = D\Theta$. The time needed for the uptake of the equilibrium curve at a defined temperature did not exceed 15 min, with total water doses at the sample surface between 300 and 1300 L, depending on temperature. After equilibrium measurements had been finished, XP spectra were recorded to determine the amount and chemical state of the remaining water. Absolute coverage determination was performed using the O1s peak area calibrated with respect to the LEED $\text{O-p}(2 \times 2)$ structure, respectively. The sample temperature was measured with a Ni/NiCr thermocouple and could be kept constant within 0.25 K during measurement.

In addition, TD-spectra were recorded with a heating rate of 2 K/s that could also verify the quality of these results.

Results and discussion of measurements on clean samples

After the adsorption of H_2O on clean Ni(1 1 1) surfaces, the XP spectra indicate only a single bonding state of oxygen with an O1s binding energy of 533.1 eV. This signal is assigned to oxygen in molecularly intact H_2O [9, 15, 16]. In the literature significantly lower binding energies are reported for the dissociation products of water [3, 17]. In contrast to the usual TPD experiments, the kinetic desorption parameters were determined by measuring the coverage in the adsorption–desorption equilibrium. In Fig. 1 equilibrium curves are shown for the clean Ni(1 1 1) surface at four different temperatures versus the adsorption flux. The coverage is normalized to the number of nickel surface atoms, i. e., at a coverage of 1 ML the number of adsorbed molecules is the same as the number of nickel atoms in the Ni(1 1 1) layer. At small gas beam intensities there is a rapid increase of coverage up to 0.42 ML. Subsequently, the coverage increases only slowly with rising adsorption flux, up to a coverage of about 0.7 ML. The abrupt increase of the curves indicates the onset of 0th order desorption, which causes a continuous multilayer growth at a H_2O flux exceeding the coverage-independent desorption rate. So an equilibrium state cannot be reached. The shape of the equilibrium curves shows that desorption energy depends on coverage. An evaluation of the equilibrium measurements in Fig. 1 gives the desorption coefficient D , and via Arrhenius the desorption energy E , and the preexponential factor ν of the

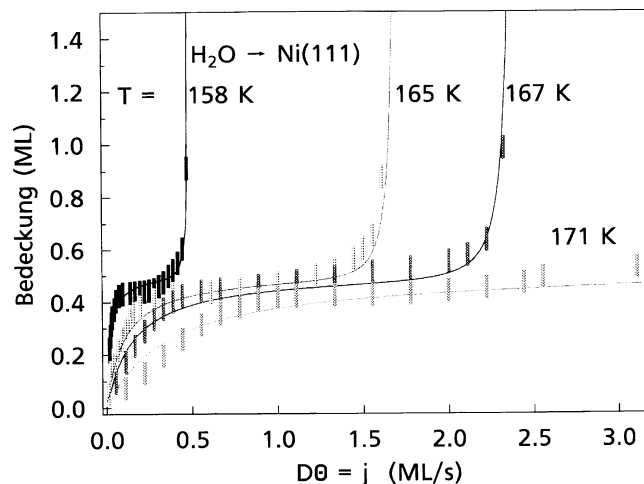


Fig. 1. Equilibrium curves of water coverage for H_2O on Ni(1 1 1) vs. H_2O beam intensity at temperatures of 158 K to 171 K

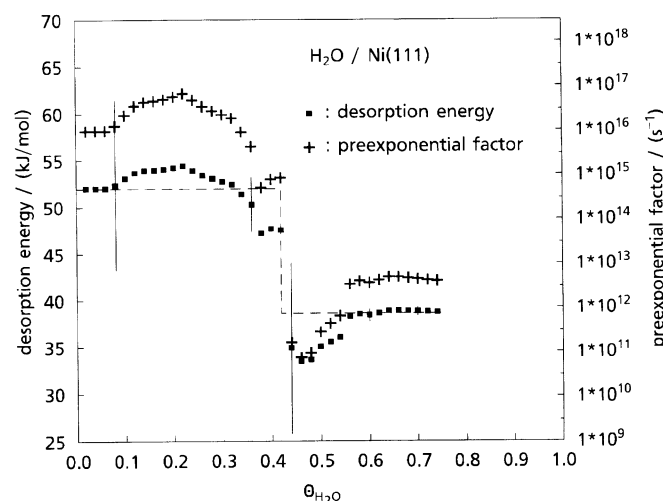


Fig. 2. Desorption energy and preexponential factor for H_2O desorption from Ni(1 1 1) vs. water coverage. The large error bars shown at low coverages result from the uncertainty in determining beam intensity. At a coverage of about 0.45 ML H_2O , they result from the uncertainty in determining the coverage. The errors of the evaluation are much lower at other coverages

desorption coefficient ($D = \nu \exp\{-E/kT\}$). At 0th order desorption the desorption flux is given by the product of the desorption coefficient D_0 and the maximum coverage Θ_{Max} on the interface which can directly exchange H_2O molecules with the gas phase.

Results from the equilibrium measurements are shown in Fig. 2 for water desorption from the pure Ni(1 1 1)-surface. On the left hand of the figure the apparent desorption energy $E_d(\Theta)$ and on the right hand the apparent preexponential factor are depicted over the water coverage, respectively. On the clean sample two adsorption states with different desorption parameters can be seen, the first at water coverages for $\Theta_{\text{H}_2\text{O}} < 0.42$ ML, exhibiting a desorption energy of $E_d = 52 \pm 3$ kJ/mol and a preexponential factor of $\nu = 10^{16 \pm 1} \text{ s}^{-1}$. For the second adsorption state for $\Theta_{\text{H}_2\text{O}} > 0.42$ ML a desorption energy of $E_d = 38.6 \pm 0.3$ kJ/mol and a preexponential

factor of $\nu = 8 \times 10^{12 \pm 0.1} \text{ s}^{-1}$ are found. The systematic errors will affect the determination of the pre-exponential factors ($\Delta\nu/\nu = 0.25$) only. The parameters for the latter are the same as the parameters determined by isothermal desorption of the ice multilayer [9, 14–16]. At $\Theta_{\text{H}_2\text{O}} > 0.42 \text{ ML}$ water desorbs with the same parameters as the multilayer up to $\Theta_{\text{H}_2\text{O}} = 0.75 \text{ ML}$; however, the desorption is 1st order. In a well-ordered ($\sqrt{3} \times \sqrt{3}R30^\circ$) bilayer structure, which for most hexagonal metal surfaces allows the best adaption for the ice lattice, coverage amounts to 0.66 ML. The ice structure seems to form already from the 2nd layer onward, which desorbs with the same kinetic data as the ice multilayer. The amount of H_2O adsorbed in this latter layer of 0.33 ML corresponds exactly to the amount of water in half a bilayer. The amount of 0.42 ML water observed here directly bonded to the nickel surface contradicts a long range well-ordered bilayer structure.

The coverage-dependent TDS measurements show two desorption peaks (for example see lowest curve in Fig. 3). One desorption peak at about 150 K can be assigned to the desorption of water with the kinetics of the ice multilayer. This peak is not observed for low H_2O coverages. It increases gradually with higher coverages. At low coverages only a desorption peak at about 163 K can be observed. This peak shows a saturation with increasing coverage. This form of desorption spectra is well-known in the literature [4, 11, 13].

From TPD and LEED measurements a maximum coverage of 0.66 ML in the first layer is observed, in our equilibrium measurements a maximum coverage of 0.42 ML was formed as first layer. A possible explanation is that in equilibrium measurements the water molecules have a high mobility on the surface and they do not exhibit a strong orientation to the surface. Due to this the water cannot build up the second half bilayer and so the coverage is lower than in a well ordered configuration.

Results and discussion of measurements on the oxygen precovered sample

Oxygen adsorbs dissociatively on Ni(1 1 1) [10, 18]. Up to a coverage of 0.33 ML, oxygen is chemisorbed. For $\Theta_{\text{O}} = 0.25 \text{ ML}$ a $p(2 \times 2)$ superstructure [19], and for $\Theta_{\text{O}} = 0.33 \text{ ML}$ a ($\sqrt{3} \times \sqrt{3}R30^\circ$) superstructure is found [20]. At the beginning of oxygen adsorption at ambient temperature no island formation occurs [21], but the formation of $p(2 \times 2)$ islands can be observed at low temperatures or at an increasing coverage [19]. At higher oxygen coverages, islands of epitaxially grown nickel oxide are formed [10, 19, 22, 23], which have an 18% higher lattice constant than nickel. With an increasing oxygen dose the NiO islands grow laterally together and form a closed epitaxial NiO(1 1 1) layer, in which about 2 ML oxygen are bonded [10, 22]. Further oxygen doses at room temperature do not lead to a further growth of the NiO layer. Both the chemisorbed oxygen and the oxygen of the nickel oxide show a signal at a binding energy of 529.3 eV in the XP spectra [15, 24, 25]. The molecular water gives an O1s signal at a binding energy of 532.7 eV.

In XP spectra a signal at 531 eV is observed for water dissociating to OH [16, 24, 25].

On oxygen precovered Ni(1 1 1), the TD spectra show three adsorption states of water (Fig. 3), of which the first desorbs at about 150 K. This state is assigned to the ice multilayer. In the following it will be named δ -state. The next adsorption state (γ -state), begins to desorb at 163 K without precovering oxygen. The desorption temperature shifts to higher temperatures with an increasing oxygen precoverage and reaches a value of 175 K at $\Theta_{\text{O}} = 0.25 \text{ ML}$. A third adsorption state (β -state) is indicated by a signal in a temperature range from 180 K to 260 K in the TD spectra [4, 5].

The δ -state is assigned to the ice multilayer also on the oxygen precovered surface and shows the same desorption parameters as on a pure Ni(1 1 1) surface. The γ -state, which is also observed on the uncovered sample, is assigned to the adsorption in the first layer on the surface. With an increasing oxygen precoverage the shift of the desorption temperature indicates altered desorption kinetics. The shift of the γ -desorption peaks with increasing oxygen precoverage is connected to an increase of desorption energy and probably depends on a long range electrostatic potential of the coadsorbed oxygen. Parallel to this shift of the TDS peak, the work function of O/Ni(1 1 1) increases linearly with Θ_{O} for coverages up to 0.3 ML [19].

On the epitaxial NiO(1 1 1) layer the desorption peak assigned to the γ -state is significantly broader than the peak of the Ni(1 1 1) surface precovered with chemisorbed oxygen. Considering the broad desorption signal, ranging

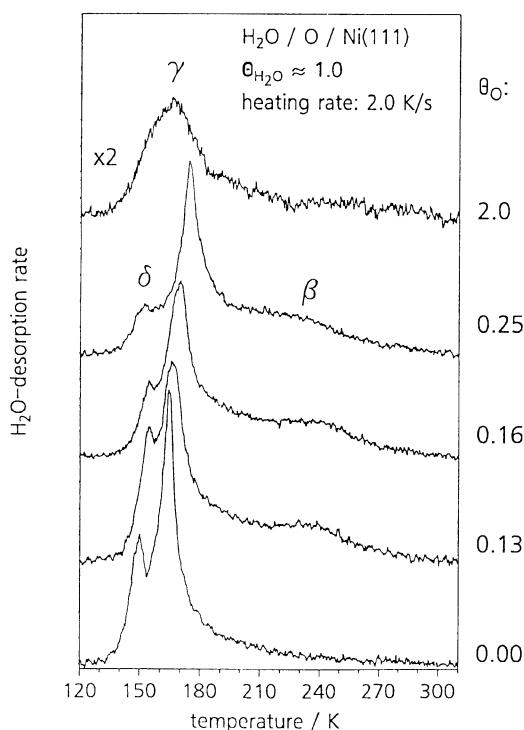


Fig. 3. TD spectra for approximately 1 ML H_2O adsorbed on the clean Ni(1 1 1) surface and on Ni(1 1 1) precovered with 0.13, 0.16, 0.25 ML of oxygen, and on a closed NiO layer

from 145 to 185 K, it seems that water does not exist in one well-defined, but rather in many different adsorption states. This may be a result of defects or domain boundaries caused by a defective adaption of the lattice between the NiO and the Ni(1 1 1) substrate. On the NiO layer the γ -peak can only be observed at water precoverages higher than 0.5 ML H_2O . A thermal desorption of H_2O from coverages below 0.5 ML can be found only at temperatures above 400 K on the NiO layer.

The width of the desorption signal in the β -state contradicts a well-ordered adsorbate structure of the water in this state. At low water coverages, on the oxygen-precovered sample this state is occupied until the H_2O coverage in the β -state is as high as the oxygen precoverage. No desorption signal is observed between 180 and 260 K in the TD spectrum of water from the NiO(1 1 1) surface. The β -water exists on energetically nonequal adsorption sites, or there is no strong interaction between H_2O molecules. This latter observation has also been made with the $\text{H}_2\text{O}/\text{K}/\text{Ni}(1 1 1)$ system [6, 26].

In the XP spectra the β -, γ - and δ -state show the same O1s binding energy, which identifies them as states of nondissociated molecular H_2O . Apart from the molecular H_2O , depending on the oxygen precoverage, another signal of oxygen from OH groups can be observed in XP spectra. This dissociated water is in the following named α -state.

To investigate the water more strongly bonded to the surface (α - and β -state), the sample was covered with 4 ML water at 156 K and kept at 156 K for 20 min without further water admission. XP spectra show that after 20 min the water (γ -state) is completely desorbed from the clean Ni(1 1 1) surface ($D_{T=156\text{ K}, \Theta=0} \approx 4 \times 10^{-2} \text{ s}^{-1}$). However, some of the water remained on the oxygen precovered surface after that period. XP spectra in Fig. 4 were obtained by subtracting the spectrum after isothermal desorption at 156 K from the spectrum of the

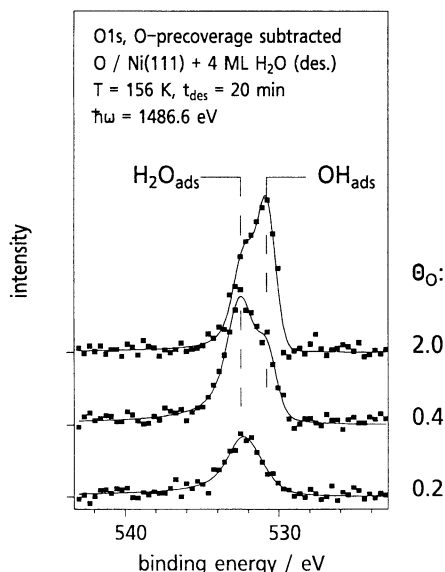


Fig. 4. O1s difference spectra at oxygen precoverages of 0.2, 0.4, and 2.0 ML. Shown in the difference between spectra before and after adsorption and thermal desorption of 4 ML of water at 156 K

oxygen precovered sample. In this way the signal of the preadsorbed oxygen does not appear in the spectra, only the signal of the additional adsorbates still present on the surface is obtained. The spectrum at an oxygen precoverage of 0.2 ML indicates that molecular water is still present on the surface. Even after a longer waiting period, it does not desorb at a temperature of 156 K, only at higher temperatures of 180 K to 260 K. Water dissociating to OH and H is not observed at an oxygen precoverage of $\Theta_{\text{O}} = 0.2$ ML, where the oxygen is present in a chemisorbed state. The XP spectra contradict the formation of 2 OH out of one H_2O and an O, as proposed by Madey et al. [13].

The curve at $\Theta_{\text{O}} = 0.4$ ML indicates the existence of molecular as well as dissociated water. At this oxygen precoverage, chemisorbed oxygen coexists with areas of NiO(1 1 1) islands on the surface. On the surface completely covered with NiO(1 1 1) there is dissociated water as well as molecular water, whereby the OH quantity amounts to about 0.5 ML and the quantity of molecular water to 0.2 ML.

Figure 5 shows the evaluation of the desorption experiment at 156 K. Depicted are the coverages of the molecular water which is bonded more strongly to the surface as compared to the clean Ni surface, and of the dissociated water versus the quantity of the preadsorbed oxygen. It can be seen that beginning at an oxygen precoverage of about 0.33 ML, where the formation of NiO islands starts, OH groups can be found. At lower oxygen precoverages only molecular water is indicated, with the coverage of water being as high as the quantity of preadsorbed oxygen. At the beginning of the nickel oxide formation, the quantity of molecular water decreases, whereas the quantity of dissociated water increases. At a coverage Θ_{O} of about 0.5 ML, the quantity of dissociated and more strongly bonded water together is as high as the quantity of preadsorbed oxygen and reaches saturation at $\Theta_{\alpha-\text{H}_2\text{O}} + \Theta_{\beta-\text{H}_2\text{O}} = 0.7$ ML for higher oxygen precoverages [4, 5, 7]. The amount of more strongly bonded molecular water found on the Ni(1 1 1) surface precovered with chemisorbed oxygen corresponds to the

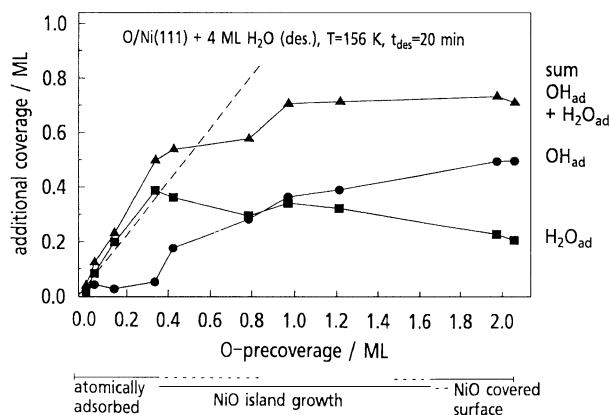


Fig. 5. Partial coverages resulting from the difference spectra of adsorbed OH and H_2O as well as the sum of both vs. the oxygen precoverage at 156 K. The dashed line gives a proportion of 1:1 of additional coverage to oxygen precoverage

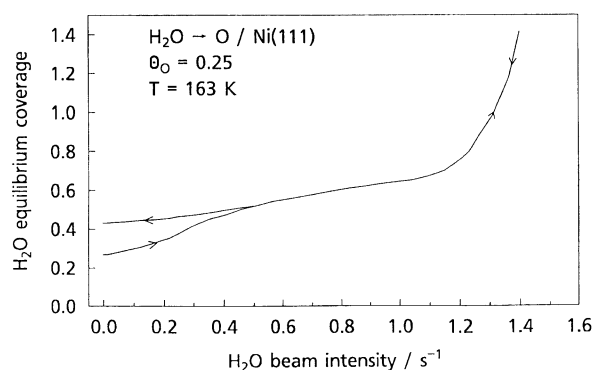


Fig. 6. Measured equilibrium curve of the water coverage on Ni(111) at an oxygen precoverage of $\Theta_{\text{O}} = 0.25$ ML and a temperature of 163 K vs. the H_2O beam intensity. The arrows show the sequence of the acquisition of the data

values found in literature [4, 5, 7]. The relation of 1:1 of the β -species to Θ_{O} indicates that in addition to bonding to the substrate there is also an interaction with the chemisorbed oxygen. This interaction causes the desorption to slow down.

Figure 6 depicts a typical coverage curve (sum of the α -, β -, γ - and δ -state) versus adsorption flux intensity in the above described equilibrium study of H_2O adsorption and desorption on the sample precovered with 0.25 ML oxygen. In contrast to the equilibrium measurements on the pure Ni(111) surface, an irreversible change of the coverage curve is obtained during the experiment. The arrows in the diagram indicate the sequence of the adsorption flux change. The adsorption flux was first increased step by step. After each pressure change, the coverage was determined when a stationary value had been reached. When the adsorption flux was sufficiently high for the ice multilayer growth or the maximum achievable adsorption flux was reached, the adsorption flux was again decreased step by step and the coverage at that pressure was determined. Running the experiment a second time, the upper curve was measured again. A slow modification of the surface during the experiment may explain this behaviour. An evaluation of kinetic data from these equilibrium measurements is impossible for small coverages (up to 0.6 ML at $\Theta_{\text{O}} = 0.25$ ML) due to these surface changes.

Conclusions

Kinetic parameters and adsorption states of water were determined on a clean Ni(111) surface by using the dynamic equilibrium between adsorption and desorption and combining this method with TDS. Evaluation of the

kinetics of water on oxygen precovered and oxidized surfaces is somewhat complicated by an irreversible surface modification during the equilibrium measurements. Nevertheless, different adsorption states could be detected for water on oxygen precovered and oxidized Ni(111) surfaces with a different dissociation behaviour. The discussion of the irreversible surface changes during equilibrium measurements will be presented in a forthcoming paper [27].

Acknowledgement. Support by the Deutsche Forschungsgemeinschaft through SFB270 is gratefully acknowledged.

References

1. Thiel PA, Madey TE (1987) *Surf Sci Rep* 7: 211
2. Memmert U, Bushby SJ, Norton PR (1989) *Surf Sci* 219: 327
3. Carley AF, Davies PR, Roberts MW, Thomas KK (1990) *Surf Sci* 238: L467
4. Pache T, Steinrück H-P, Huber W, Menzel D (1989) *Surf Sci* 224: 195
5. Bornemann T (1991) Dissertation, Technische Universität München
6. Kuch W, Schnurnberger W, Schulze M, Bolwin K (1994) *J Chem Phys* 101: 1687
7. Nöbl C, Benndorf C (1987) *Surf Sci* 182: 499
8. Benndorf C, Mundt C (1992) *J Vac Sci Technol A* 10: 3026
9. Kuch W, Schulze M, Schnurnberger W, Bolwin K (1993) *Ber Bunsenges Phys Chem* 97: 356
10. Norton PR, Tapping RL, Goodale JW (1977) *Surf Sci* 65: 13
11. Stulen RH, Thiel PA (1985) *Surf Sci* 157: 99
12. Zakharov II, Avdeev VI, Zhidomirov GM (1992) *Surf Sci* 277: 407
13. Madey TE, Netzer FP (1982) *Surf Sci* 117: 549
14. He J-W, Norton PR (1990) *Surf Sci* 238: 95
15. Kuch W (1993) Dissertation, Universität Stuttgart
16. Fischer M, Schnurnberger W, Schulze M, Kuch W, Kienzlen V (1991) In: *Energieträger Wasserstoff* VDI-Verlag, Düsseldorf
17. Fuggle JC, Watson LM, Fabian DJ, Affrossman S (1975) *Surf Sci* 49: 61
18. Wandelt K (1982) *Surf Sci Rep* 2: 1
19. Kortan KR, Park RL (1981) *Phys Rev B* 23: 6340
20. Mendez MA, Oed W, Fricke A, Hammer L, Heinz K, Müller K (1991) *Surf Sci* 253: 99
21. MacRae AU (1964) *Surf Sci* 1: 319
22. Holloway PH, Hudson JB (1974) *Surf Sci* 43: 141
23. MacRae AU (1963) *Appl Phys Lett* 2: 88
24. Cappus D, Xu C, Ehrlich D, Dillmann B, Ventrice CA Jr, Al-Shamery K, Kühlenbeck H, Freund H-J (1993) *Chem Phys* 177: 533
25. Winkelmann F, Wohlrab S, Libuda J, Bäumer M, Cappus D, Menges M, Al-Shamery K, Kühlenbeck H, Freund H-J (1995) *Surf Sci* (in press)
26. Kuch W, Schulze M, Schnurnberger W, Bolwin K (1993) *Surf Sci* 287/288: 600
27. Schulze M, Kuch W, Reißner R, Bolwin K, In preparation